Noncritical Slowing Down of Photonic Condensation

Benjamin T. Walker,[1,2] Henry J. Hesten,[1,2] Himadri S. Dhar,[1] Robert A. Nyman,[1] and Florian Mintert[1]
[1]Physics Department, Blackett Laboratory, Imperial College London, Prince Consort Road, London SW7 2AZ, United Kingdom
[2]Centre for Doctoral Training in Controlled Quantum Dynamics, Imperial College London, Prince Consort Road, SW7 2AZ, United Kingdom

(Received 24 September 2018; published 13 November 2019)

We investigate the response of a photonic gas interacting with a reservoir of pumped dye molecules to quenches in the pump power. In addition to the expected dramatic critical slowing down of the equilibration time around phase transitions, we find extremely slow equilibration even far away from phase transitions. This noncritical slowing down can be accounted for quantitatively by fierce competition among cavity modes for access to the molecular environment, and we provide a quantitative explanation for this noncritical slowing down.

DOI: 10.1103/PhysRevLett.123.203602

The timescales of evolution of simple dynamical systems are typically directly related to system parameters. By contrast, systems with many degrees of freedom can exhibit emergent behavior, with dynamics on timescales that have no clear origin in the microscopic equations of motion. A prominent example is the relaxation towards a steady state which is known to slow down when a system is close to a critical point [1,2]. This critical slowing down is present in the statistical mechanics of systems from atomic quantum gases [3] or magnetic metamaterials [4] to entire ecosystems or human societies [5].

The slowing down of system dynamics goes hand in hand with an increase in the amplitude of the fluctuations in both classical [6] and quantum statistical systems [7]. Close to criticality, fluctuations and dynamics become linked, and the system behavior can be characterized by critical exponents [1,8]. In this respect, critical slowing down is a very different phenomenon from other delayed-equilibrium phenomena such as prethermalization of isolated quantum gases [9] or light [10], and Anderson localization [11]. Noncritical slowing down is typically related to the integrability of the dynamical variables or to the kinetic impossibility of exploring the full state space available, and therefore not directly linked to fluctuations.

In this Letter, we investigate the slowing down of equilibration in a photonic gas in a pumped, dye-filled optical microcavity. Far from critical pump parameters, the response of the photon populations to abrupt changes in pumping has been shown experimentally to occur on timescales typical for the absorption of a cavity photon by a dye molecule [12,13]. The fluctuations of photon numbers [14] and the phase of a Bose-Einstein condensate [15,16] have been observed to occur on similar timescales. Here, we find both critical and noncritical slowing down. Unusually, the noncritical slowing down does not appear to be related to an impossibility of exploring the state space but rather to a detailed balance of excitations being exchanged between photon modes and partially overlapping subsets of the dye molecules. Furthermore, it is connected to an inversion of an important susceptibility of the system (derivative of photon number in a specific mode with respect to pump power), implying a very unusual relationship between equilibration and fluctuation.

The system dynamics is described well in terms of rate equations for the occupations n_i of cavity modes and a vector f characterizing the inhomogeneous fractional excitation of all dye molecules [17]. A suitable construction of collective modes of molecular excitations [18] enables the reduction of the molecular environment to its most relevant degrees of freedom. To this end, the vector f is decomposed into a hierarchy of several components $f_j = \mathcal{P}_j f$ with suitably defined projectors $\mathcal{P}_j$. By construction the cavity dynamics depends only on the level-0 component f_0, and the level-$(j+1)$ component f_{j+1} affects the cavity dynamics only indirectly via its influence on the level-j component f_j. A truncation after two or three levels provides an excellent description of the system dynamics with substantial gain in numerical efficiency [18].

The level-0 component f_0 can be expanded into a set of vectors $\mathbf{e}_i$ such that the equation of motion [17,18]

$$\dot{n}_i = [n_i(E_i + A_i) + E_i]c_i v_i - \gamma_i n_i \tag{1}$$

for each occupation number n_i of a cavity mode depends only on the single component $v_i = \mathbf{e}_i^T f_0$ of the molecular environment. The corresponding coupling constant c_i reads $c_i = \sum_j g_{ij} M_j [\mathbf{e}_i]_j$, where g_{ij} is the coupling constant between cavity mode i and a dye molecule at position j; M_j is the number of molecules in the small volume element around this position, and $[\mathbf{e}_i]_j$ is the element j of the vector $\mathbf{e}_i$. A_i and E_i are the rates of absorption and emission of a

dye molecule, and $\gamma_i = A_i \sum_j g_{ij} M_j + \kappa$ is the decay constant, including the cavity decay rate κ.

The equations of motion for the excited state fractions of molecules f_j read

$$\dot{f}_j = \sum_k \sum_i n_i \mathcal{P}_j B_i \mathcal{P}_k f_k - B_0 f_j - \mathcal{P}_j x, \qquad (2)$$

in terms of the diagonal matrices B_i with diagonal elements $[B_i]_{pp} = -(E_i + A_i) g_{ip}$, the matrix $B_0 = \sum_i B_i E_i / (E_i + A_i) + (\Gamma_\downarrow + P)\mathbf{1}$, the vector x with elements $[x]_j = P + \sum_i g_{ij} A_i n_i$, the pump rate P, and the decay constant $\Gamma_\downarrow$ for nonradiative decay or emission into free space [17,18].

This approach allows us to investigate the equilibration of the light in the cavity after quenches in pump power. Strictly speaking, a steady state is reached only asymptotically, but in practice, one can accept small deviations and thus define a finite time to reach stationarity. We deem stationarity to be reached if the difference between populations of current state and exact steady state reaches a specified fraction of the exact steady state population for each mode of the cavity. The specification of this fraction is largely arbitrary; we chose a value of 10^{-6}, and a different choice would result in an overall change of timescale.

We consider a two-dimensional cavity with parabolic mirrors and harmonic oscillator eigenmodes labeled with the double index $i = [m_x, m_y]$. We take into account the lowest five energy levels, corresponding to 15 photonic cavity modes. In the Supplemental Material [19] we show that the numerical results for these parameters are unchanged for larger numbers of modes with a fixed number of molecules. Expressing all system parameters in units of cavity decay constant κ and the harmonic oscillator length l_{ho}, we use a molecular density of $10^{13}/l_{ho}^2$, $M_j = 10^{12}$ molecules in each group and a molecular decay rate $\Gamma_\downarrow = \kappa/4$; the absorption and emission rates are $A_{[m_x,m_y]} = 10^{-12}\kappa[3.8, 9.2, 23.0, 55.4, 124.9]_{m_x+m_y}$, and $E_{[m_x,m_y]} = 10^{-10}\kappa[5.6, 6.8, 8.2, 9.3, 10.0]_{m_x+m_y}$, respectively, matching that of rhodamine 6G.

In order to analyze the equilibration time, we start with the system in its stationary state at a given pump power and then increase the pump power with a quench of 1%. Figure 1 (top) shows the time taken to reach the steady state after this quench as a function of postquench pump power; the bottom panel shows the corresponding steady state population in each mode at the final pump power. One can see clear peaks in equilibration time at pump powers at which cavity modes condense or decondense. The intervals below and between the phase transitions seen in Fig. 1 (top) are labeled by letters A to E. In the intervals A to C, the equilibration time is about a factor of 10 larger than the cavity decay time $1/\kappa$. In interval D, however, the equilibration time does not reduce to the values found in A to C, and interval E features a broad

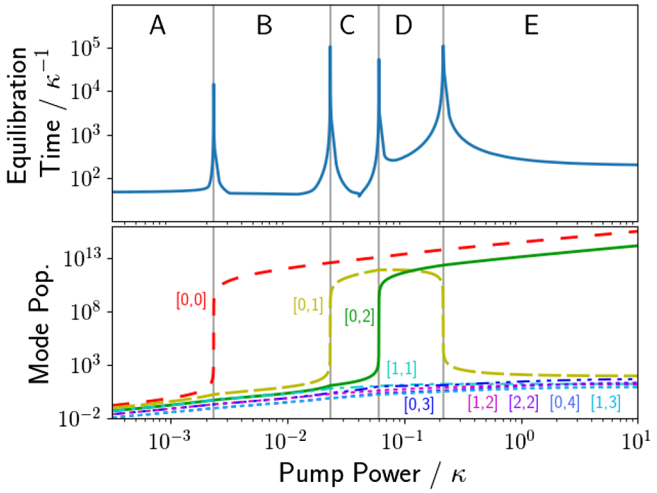

FIG. 1. Top: time taken for the system to equilibrate after a quench in pump power by 1%, as a function of the pump power after the quench. Bottom: steady state populations n_i of cavity modes i ranging from [0, 0] to [1, 2] and [0, 3]. The mode populations feature sharp increases and drops under increase of pump power, and the equilibration times show clear peaks around those phase transitions. In addition to this, the equilibration is also strongly slowed down in the intervals labeled D and E far away from any known phase transition.

plateau of the equilibration time, more than an order of magnitude larger than the base value around $10/\kappa$. We explicitly verify that this plateau extends to pump rates reaching $10^3\kappa$, and that for parameters where a further condensation peak is observed, the noncritical slowing is not dependent on the tails of a subsequent condensation peak (see the Supplemental Material [19]).

Critical slowing down around phase transitions is well known [3–5], and we find that all four phase transitions are characterized by the same critical exponent of 1, i.e., a divergence of the equilibration time $\propto |P - P_c|^{-1}$ as the pump power P reaches its critical value P_c. In contrast to this well-known critical slowing down, however, the increase of equilibration time in D and E is not associated with any phase transition. To the best of our knowledge, such *noncritical* slowing has never been observed, and quite strikingly the timescale of more than $10^2/\kappa$ does not match any of the natural timescales of the system.

Both the fast and the slow equilibration times can be explained in terms of Eq. (1). Photons are being lost from the system with rate κ, and since the exchange of photons between cavity and environment is faster than this loss process, the system relaxes to the new steady state with a decay constant close to κ after the change in pump power. Assuming an exponential decay, the relative deviation δn_i from the steady state has decayed to a value of d after the time t_e satisfying $\delta n_i \exp(-\kappa t_e) = d$. With the value of $\delta n_i = 2\%$ that we find for a quench by 1% sufficiently far away from the phase transitions, and the threshold $d = 10^{-6}$, one would

thus expect an equilibration time of $t_e = -\ln(5\times10^{-5})/\kappa \simeq 10/\kappa$ which matches the observed values very well.

The slowing down of equilibration time can be attributed to the fact that the molecular excitation v_i remains close to its critical value despite the quench in pump power. If this is the case, it is convenient to reexpress Eq. (1) as

$$\dot{n}_i = -(E_i + A_i)(v_i^c - v_i)n_i + E_i v_i, \tag{3}$$

in terms of the critical excitation $v_i^c = \gamma_i/(E_i + A_i)$ for which the stationary state solution of Eq. (1) diverges. If v_i remains constant, one can understand $\eta_i = (E_i + A_i)(v_i^c - v_i)$ as the effective decay rate, and whenever the dye excitation v_i approaches its critical excitation $v_i^{(c)}$, the effective rate η_i becomes minute and the dynamics of mode i slows down.

Consistent with critical slowing down, the condition $v_i \lesssim v_i^{(c)}$ is typically satisfied close to a phase transition, even after a quench in pump power. Far away from a phase transition, any quench in pump power causes v_i to differ substantially from its critical value so that regular equilibration on the timescale κ applies, but as one can see in Fig. 1 this does not hold in the intervals D and E.

In order to understand why the excitations $v_{[0,1]}$ in the molecular environment that are accessible to the cavity mode [0, 1] hardly react to quenches in pump power in the intervals D and E, but not in any of the other intervals, one has to inspect the effect of clamping caused by the condensed modes. Given the macroscopic occupation of condensed modes, the coupling between those modes and the molecular environment is extremely strong. If this coupling is so strong that the interaction between a molecule and the external pumping becomes negligible, this molecule will not increase its excitation as pumping is increased, and it is considered to be clamped to the condensed mode [17,20].

The mode vectors $\mathbf{e}_i$ that describe the spatial excitation profile to which the modes i couple, share similarities with the spatial profile of the cavity modes, as one can see in Fig. 2, where the mode profiles for the three lowest eigenstates of a harmonic oscillator and the corresponding excitation profiles $\mathbf{e}_i$ are depicted. Since those profiles coincide with one-dimensional cuts through the excitation profiles $\mathbf{e}_{[0,i]}$, Fig. 2 provides a physical picture of how clamping causes slow equilibration in D and E, but not in the other intervals depicted in Fig. 1. Crucially, unlike the photonic cavity modes, the excitation profiles are *not* mutually orthogonal, and their dynamics are coupled as described by Eq. (2). This means that a cavity mode can clamp other excitation profiles as well as its own. As one can see, the cavity mode profile of the mode [0, 1] has two maxima around which it couples strongly to the molecular environment (opaque regions G1 in Fig. 2). The mode [0, 0] couples strongly in the region C0 between those maxima, and the mode [0, 2] couples strongly between and outside those two maxima as indicated by C2. There are thus

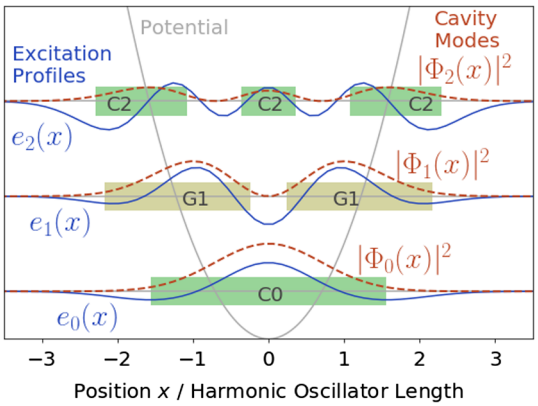

FIG. 2. Moduli squares $|\Phi_i(x)|^2$ for $i = 0, 1, 2$ of the three lowest eigenfunctions of a quantum harmonic oscillator are depicted in red. The corresponding harmonic potential and lines indicating the eigenenergies are depicted in grey. The excitation profile functions $\mathbf{e}_i(x)$ corresponding to each of these cavity modes are depicted in blue. Green bars (C0 and C2) approximate one-dimensional cuts through the areas in which modes [0, 0] and [0, 2] compete for excitations and clamp molecules when condensed. Yellow bars (G1) denote the approximate locations of molecules absorbing photons from or emitting photons into mode [0, 1]. Mode [0, 1] experiences competition through the whole of G1 with either [0, 0] or [0, 2].

regions in which the competition between mode [0, 1] and the modes [0, 0] and [0, 2] for access to the excitations of the dye molecules is particularly strong. In the intervals B and C, where mode [0, 0] is condensed, the molecules in C0 —in particular in the overlap with G1—can become clamped, but the molecules outside the maxima can still change their excitation sufficiently well in response to a quench in pump, to allow for equilibration on the regular timescale. In the intervals D and E, mode [0, 2] can also contribute to the clamping, so that the molecules on both sides of the relevant domain—including the overlap between G1 and C2—are being clamped. This then results in the stabilization of $v_{[0,1]}$ close to $v_{[0,1]}^c$ and the corresponding slow equilibration, even though the driving pump has good overlap with all molecular excitation profiles.

In order to substantiate that Eq. (3) indeed describes well the slow equilibration, stronger quenches than 1% are more informative, since these will result in pronounced dynamics of the cavity excitation which allows for stringent comparison with the analytic prediction. Figure 3 shows in detail the dynamics of a slow equilibration process resulting from an increase in pump power by 3 orders of magnitude. One can see that the population $n_{[0,0]}$ of the ground-state mode grows monotonically as result of the quench and that it reaches its new steady state on the timescale $10/\kappa$. The population $n_{[0,2]}$ also reaches its new steady state quickly, though not monotonically. The population $n_{[0,1]}$ of the first excited mode rapidly grows to a value 14 orders of magnitude larger than its stationary

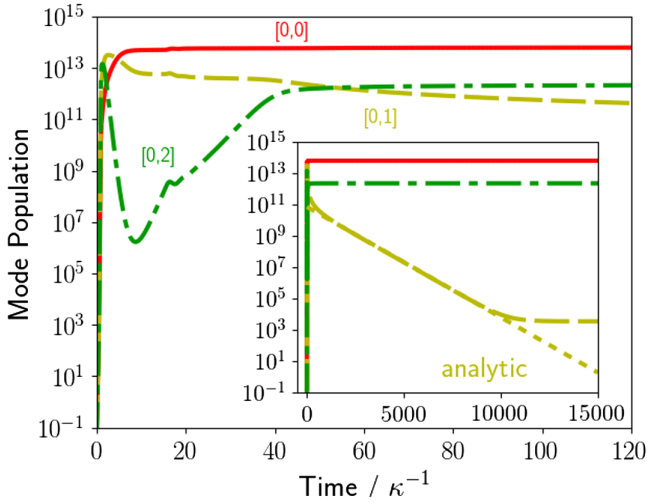

FIG. 3. Mode populations as a function of time after a quench in pump power from $3.16 \times 10^{-4}\kappa$ to $2.5 \times 10^{-1}\kappa$. Modes [0, 0] and [0, 2] reach their new steady state on a timescale of $10/\kappa$, but equilibration of mode [0, 1] is about 3 orders of magnitude slower. The dotted line depicts the analytic prediction of Eq. (3), that matches the simulated data very well over a range of 7 orders of magnitude. In this case, the equilibration time is determined by the dynamics of mode [0, 1].

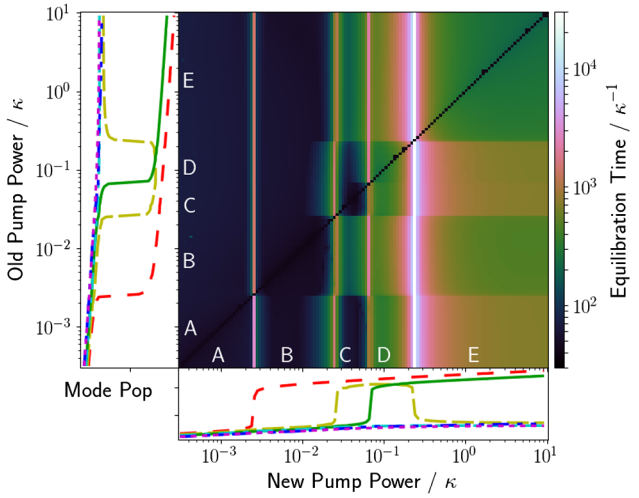

FIG. 4. Time taken to reach steady state after the pump power is changed from the value indicated at the left to the value depicted at the bottom of the figure. The axes also depict the stationary state populations for the lowest three cavity modes as also shown in Fig. 1 and the division into intervals A to E. One can see a clear enhancement of equilibration time close to the phase transitions, but also in the interval D and E of postquench pump power.

value, but then reaches its new steady state on a substantially longer timescale. In the time window between $10/\kappa$ and $10^3/\kappa$ the decay is approximately algebraic $\propto t^{-\frac{3}{2}}$. The inset depicts dynamics on a timescale 2 orders of magnitude larger than the main figure, and confirms the subsequent exponential decay predicted by Eq. (3) with $v_{[0,1]}$ taken from the stationary solution. The nearly perfect agreement with the simulated data over 7 orders of magnitude strongly supports the explanation of slow equilibration resulting from the close-to-critical value of $v_{[0,1]}$.

The situation depicted in Fig. 3 is not specific to the chosen values of the pump power, but rather generic, as one can see in Fig. 4, where the equilibration time is shown as a function of pump power before and after a quench. The vertical lines separating the intervals A to E show that the equilibration time around phase transitions is slow, independent of the initial state. Also equilibration within the intervals A, B, and C is fast for any initial pump power. Equilibration in the intervals D and E is always slow, and it tends to be slower in E than in D consistent with the reaction to the small quenches depicted in Fig. 1. Quite surprisingly, however, the equilibration time for a postquench state in D or E does depend on the initial conditions to some extent. In particular, for initial conditions in B, equilibration is less slow in E, and particularly slow in D. This can be attributed to the fact that, after a quench from initial conditions in A, mode [0, 1] gains macroscopic occupation of approximately 10^{13} before being clamped by modes [0, 0] and [0, 2], as shown in Fig. 3. After a quench from phase B, however, mode [0, 0] is already macroscopically occupied and immediately clamps mode [0, 1], which only attains a population of 10^7 before being clamped by modes [0, 0] and [0, 2]. This reduction in the population of mode [0, 1] reduces the time taken to decay to the steady state in E, but increases the time taken to reach the macroscopic occupation of region D.

This effect can also be exploited in order to arrive at steady states faster than with a simple quench. Starting with a pump power corresponding to interval A, for example, and quenching to interval E will require an equilibration time about a factor of 2 longer than with a quench to interval B followed by a quench to interval E after a short delay. This effect is just a first signature of the vast potential that temporally modulated pumping has for the control of nonequilibrium phases of light. Varying pump powers without waiting for full equilibration will give access to the interplay of dynamics on fundamentally different timescales that can, for example, be used to let undesired features decay while desired features are protected by slow decay times. Together with the ability to change the effective interactions between different cavity modes in terms of suitably shaped cavity modes [21] this opens entirely new avenues towards the creation of tailored states of light with abundant applications such as quantum simulations or precision sensing. These ideas are by no means limited to bright sources of light, as considered here, but it applies equally well to systems with microfabricated cavities that support condensation of a few tens of photons [22] or even below ten photons [15]. In such systems, suitably chosen temporal profiles of pumping can also be used to explore quantum states with variable intermode

correlations and coherence properties and the suppressed interaction with the molecular environment identified here can protect such nonclassical states against decoherence and decay.

We are indebted to Andre Eckardt, Alex Leymann, and Rupert Oulton for stimulating discussions. Financial support through UK-EPSRC in terms of the Grants No. EP/312 J017027/1, No. EP/S000755/1 and the Centre for Doctoral Training Controlled Quantum Dynamics No. EP/L016524/1, and through the European Union's Horizon 2020 research and innovation programme under grant agreement No. 820392 (PhoQuS), is gratefully acknowledged.

[1] P. C. Hohenberg and B. I. Halperin, Theory of dynamic critical phenomena, Rev. Mod. Phys. **49**, 435 (1977).
[2] M. Suzuki, K. Kaneko, and F. Sasagawa, Phase transition and slowing down in non-equilibrium stochastic processes, Prog. Theor. Phys. **65**, 828 (1981).
[3] R. Labouvie, B. Santra, S. Heun, and H. Ott, Bistability in a Driven-Dissipative Superfluid, Phys. Rev. Lett. **116**, 235302 (2016).
[4] L. Anghinolfi, H. Luetkens, J. Perron, M. G. Flokstra, O. Sendetskyi, A. Suter, T. Prokscha, P. M. Derlet, S. Lee, and L. J. Heyderman, Thermodynamic phase transitions in a frustrated magnetic metamaterial, Nat. Commun. **6**, 8278 (2015).
[5] V. Dakos and J. Bascompte, Critical slowing down as early warning for the onset of collapse in mutualistic communities, Proc. Natl. Acad. Sci. U.S.A. **111**, 17546 (2014).
[6] K. Kawasaki, Kinetic equations and time correlation functions of critical fluctuations, Ann. Phys. (N.Y.) **61**, 1 (1970).
[7] L. W. Clark, L. Feng, and C. Chin, Universal space-time scaling symmetry in the dynamics of bosons across a quantum phase transition, Science **354**, 606 (2016).
[8] N. Navon, A. L. Gaunt, R. P. Smith, and Z. Hadzibabic, Critical dynamics of spontaneous symmetry breaking in a homogeneous Bose gas, Science **347**, 167 (2015).
[9] M. Gring, M. Kuhnert, T. Langen, T. Kitagawa, B. Rauer, M. Schreitl, I. Mazets, D. A. Smith, E. Demler, and J. Schmiedmayer, Relaxation and prethermalization in an isolated quantum system, Science **337**, 1318 (2012).
[10] N. Šantić, A. Fusaro, S. Salem, J. Garnier, A. Picozzi, and R. Kaiser, Nonequilibrium Precondensation of Classical Waves in Two Dimensions Propagating through Atomic Vapors, Phys. Rev. Lett. **120**, 055301 (2018).
[11] J. Billy, V. Josse, Z. Zuo, A. Bernard, B. Hambrecht, P. Lugan, D. Clément, L. Sanchez-Palencia, P. Bouyer, and A. Aspect, Direct observation of Anderson localization of matter waves in a controlled disorder, Nature (London) **453**, 891 (2008).
[12] J. Schmitt, T. Damm, D. Dung, F. Vewinger, J. Klaers, and M. Weitz, Thermalization kinetics of light: From laser dynamics to equilibrium condensation of photons, Phys. Rev. A **92**, 011602(R) (2015).
[13] T. K. Hakala, A. J. Moilanen, A. I. Väkeväinen, R. Guo, J.-P. Martikainen, K. S. Daskalakis, H. T. Rekola, A. Julku, and P. Törmä, Bose–Einstein condensation in a plasmonic lattice, Nat. Phys. **14**, 739 (2018).
[14] J. Schmitt, T. Damm, D. Dung, F. Vewinger, J. Klaers, and M. Weitz, Observation of Grand-Canonical Number Statistics in a Photon Bose-Einstein Condensate, Phys. Rev. Lett. **112**, 030401 (2014).
[15] B. T. Walker, L. C. Flatten, H. J. Hesten, F. Mintert, D. Hunger, A. A. P. Trichet, J. M. Smith, and R. A. Nyman, Driven-dissipative non-equilibrium Bose–Einstein condensation of less than ten photons, Nat. Phys. **14**, 1173 (2018).
[16] J. Schmitt, T. Damm, D. Dung, C. Wahl, F. Vewinger, J. Klaers, and M. Weitz, Spontaneous Symmetry Breaking and Phase Coherence of a Photon Bose-Einstein Condensate Coupled to a Reservoir, Phys. Rev. Lett. **116**, 033604 (2016).
[17] J. Keeling and P. Kirton, Spatial dynamics, thermalization, and gain clamping in a photon condensate, Phys. Rev. A **93**, 013829 (2016).
[18] B. T. Walker, H. J. Hesten, R. A. Nyman, and F. Mintert, companion paper, Phys. Rev. A **100**, 053828 (2019).
[19] See Supplemental Material at http://link.aps.org/supplemental/10.1103/PhysRevLett.123.203602 for additional analysis related to the phenomenon of noncritical slowing in photon condensates presented in this Letter.
[20] H. J. Hesten, R. A. Nyman, and F. Mintert, Decondensation in Nonequilibrium Photonic Condensates: When Less Is More, Phys. Rev. Lett. **120**, 040601 (2018).
[21] L. Flatten, A. Trichet, and J. Smith, Spectral engineering of coupled open-access microcavities, Laser Photonics Rev. **10**, 257 (2016).
[22] D. Dung, C. Kurtscheid, T. Damm, J. Schmitt, F. Vewinger, M. Weitz, and J. Klaers, Variable potentials for thermalized light and coupled condensates, Nat. Photonics **11**, 565 (2017).